AJNR

A Novel Method to Measure Venular Perivascular Spaces in Patients with MS on 7T MRI

I.C. George, A. Arrighi-Allisan, B.N. Delman, P. Balchandani, S. Horng and R. Feldman

A Novel Method to Measure Venular Perivascular Spaces in Patients with MS on 7T MRI

I.C. George, A. Arrighi-Allisan, B.N. Delman, P. Balchandani, S. Horng, and R. Feldman

ABSTRACT

SUMMARY: In MS, inflammatory cells accumulate within the perivascular spaces of acute and chronic lesions. Reliance on perivascular spaces as biomarkers for MS remains uncertain because various studies have reported inconsistencies in perivascular space anatomy. Distinguishing between venular and arteriolar perivascular spaces is pathophysiologically relevant in MS. In this pilot study, we leverage susceptibility-weighted imaging at 7T to better identify perivascular spaces of venular distribution on corresponding high-resolution T2 images.

ABBREVIATIONS: HC = healthy controls; PVS = perivascular space

In MS, immune cells, immunoglobulins, and proinflammatory factors cross 2 barriers to enter the CNS: the vascular endothelium, or blood-brain barrier, and the glia limitans.[1] Between these is the perivascular space (PVS), where immune cells may accumulate in both active and chronic MS lesions.[2]

The localization of immune cells and inflammatory markers in relation to perivascular spaces, along with formation of MS lesions around central veins, suggests that changes in PVS anatomy may reflect disease severity.[3] Previous work reported differences in the PVS anatomy between patients with MS and healthy controls (HC), though results have conflicted.[4-6] In addition to the heterogeneities of the study design, including differences in field strengths and MS phenotypes, discrepancies may relate to inadequate differentiation between venular and arteriolar PVSs, which are differentially affected in MS.[7] We hypothesized that selective analysis of venular PVSs may more accurately reflect pathophysiologic changes in MS.

We developed a novel technique coregistering T2-TSE images with SWI to identify venular PVSs (with central susceptibility suggesting deoxygenated blood) or nonvenular PVSs (lacking susceptibility). We present the pilot results at 7T on 3 persons with relapsing-remitting MS and 3 HC.

MATERIALS AND METHODS

Three persons with MS (1 woman/2 men; Expanded Disability Status Scale scores, 2.0, 3.0, and 0; 32, 33, and 35 years of age) and 3 age-matched HC (32, 33, and 35 years of age) were recruited through Mount Sinai Hospital. All persons with MS met the 2017 McDonald criteria[8] and received disease-modifying therapy. Informed consent was obtained from all participants.

Subjects were scanned on a 7T scanner (Magnetom 7T; Siemens) using an SC72CD gradient coil (maximum slew rate = 200 T/m/s, Gmax = 70 mT/m) with single-channel transmit and 32-channel receive head coils (Nova Medical). Sequences included T2-TSE, SWI, and MP2RAGE with a uniform denoised reconstruction. Details are listed in the protocol.[9]

To detect vessels, we developed a vessel-segmentation tool in Matlab (MathWorks).[10] Minimum-intensity-projection images were obtained from SWI. Vessel edge enhancement was performed by finding the eigenvalues of the Hessian matrix.[11,12]

Uniform denoised images were used to create GM and WM volumetric segmentations of the brain using FreeSurfer, Version 6.0. (http://surfer.nmr.mgh.harvard.edu). Segmentations were used to calculate total WM volume and create GM and WM masks. Lesions were segmented by the lesion growth algorithm (https://
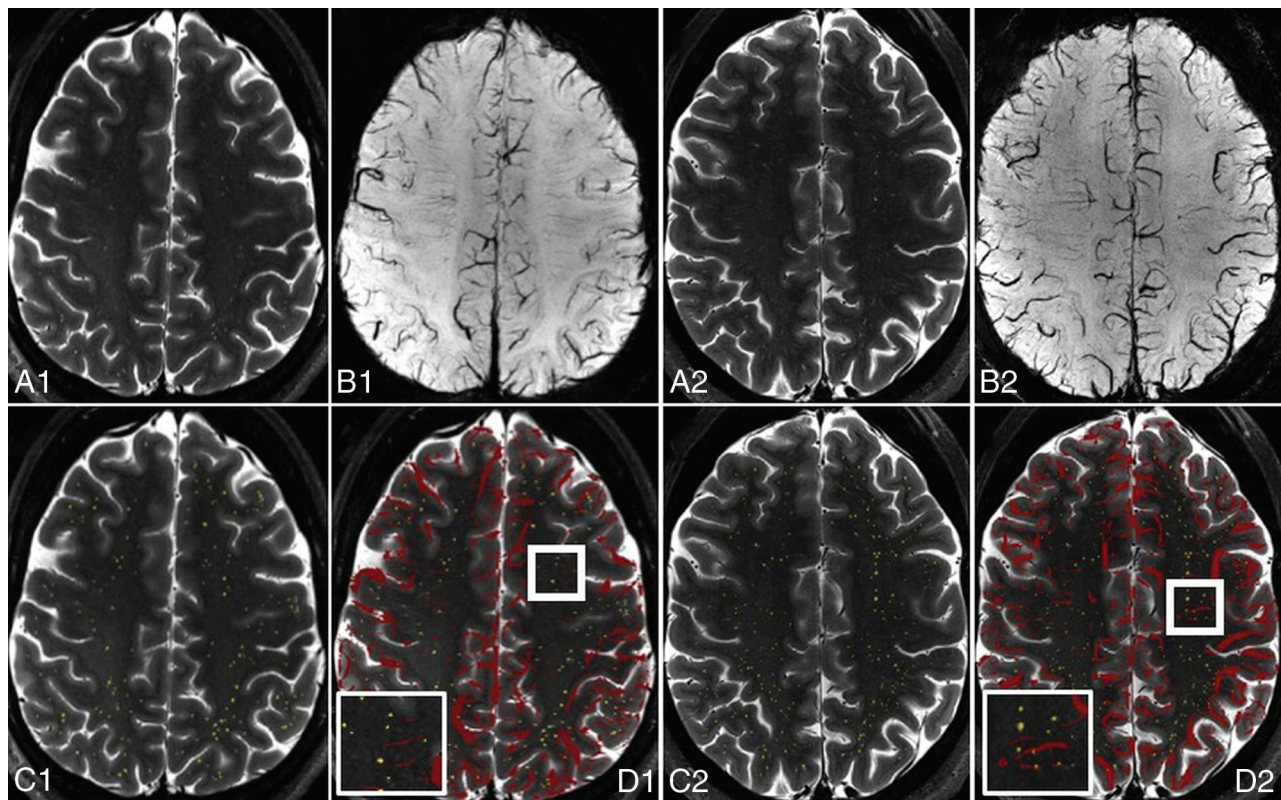
FIG 1. Overlay of pre- and postprocessed images of T2-TSE with manual PVS markings and SWI at 7T in a healthy control (*A–D* 1) and a person with MS (*A–D* 2) allows identification of venular and nonvenular PVSs. T2-TSE (*A*), SWI (*B*), T2-TSE with PVSs highlighted in yellow (*C*), and T2-TSE with SWI overlay in red (*D*) are depicted, with magnification of 1 sample area in the *thick white square* demonstrated in the thinner *white square inset*.

www.applied-statistics.de/lst.html).[13] The uniform denoised, T2-TSE, and susceptibility-weighted images were coregistered using SPM12 (http://www.fil.ion.ucl.ac.uk/spm/software/spm12), and the FreeSurfer-derived masks were used to isolate WM of the cerebral hemispheres.

The resulting 3D datasets were connected along an 18-connected network through the nearest neighbors. Individual objects were characterized using the "bwlabel" function in Matlab, and principal axes were extracted. Networks were filtered to exclude objects with a major-/minor-axis length ratio of <4, to eliminate nonvessel punctate foci of susceptibility.

For all subjects, WM PVSs were manually marked on coregistered T2-TSE images by 2 raters (I.C.G. and A.A.-A.) on OsiriX Imaging Software, Version 9.0.2 (http:// www.osirix-viewer.com). An individual ROI was identified for each marked PVS. PVSs were marked on the diameter through the short axis of the ROI (excluding diameters of <0.5 mm). Gray matter and posterior fossa PVSs were excluded because these areas are prone to artifacts at 7T. Interrater reliability was assessed comparing total PVSs marked per section by each reviewer.

Vessel and PVS masks were overlaid to quantify the coincidence of PVSs and segmented veins relative to the total number of detected PVSs. Total numbers of PVSs and venular PVSs were averaged across raters for persons with MS and HC.

A percentage perivenular space quotient was calculated for each subject by dividing the number of venular spaces detected by the total number of perivascular spaces. A nonparametric

Moods median test was performed to compare this percentage in HC versus persons with MS. A χ^2 test of independence was performed to assess the relationship between the number of venular PVSs and total PVSs in HC and persons with MS.

RESULTS
Alignment of PVSs manually marked on T2-TSE sequences with corresponding SWI demonstrated the feasibility of this approach (Fig 1).

Interrater reliability was high between reviewers, demonstrating correlation coefficients of $r = 0.95$ and $r = 0.85$ on 2 scans.

The total PVS number and percentage of venular PVSs were quantified for 3 persons with MS and 3 HC. The mean total PVSs were 4976 (SD, 282.6) in persons with MS versus 8487 (SD, 2645.1) in HC ($P = .15$). Of these, 15.19% were venular in the persons with MS group versus 10.26% venular in HC ($P = .014$) (Fig 2). In this sample, even though persons with MS had fewer detectable perivascular spaces than HC, a larger proportion of spaces in persons with MS were venular. Total brain volumes and WM volumes were similar between the persons with MS and HC, with a mean total volume of 1162 mL (range, 968–1319 mL) in persons with MS and 1042 mL (range, 996–1101 mL) in HC (t test, $P = .46$). Mean WM volume was 470 mL (range, 374–557 mL) in patients with MS and 444 mL (range, 441–449 mL) in HC (t test, $P = .68$). Mean lesion volume was 1.3 mL (range, 0.45 –1.45 mL).

In HC, the number of venular PVSs was highly related to the number of PVSs ($\chi^2 = 0.26$, 2 *df*), while in the persons with MS
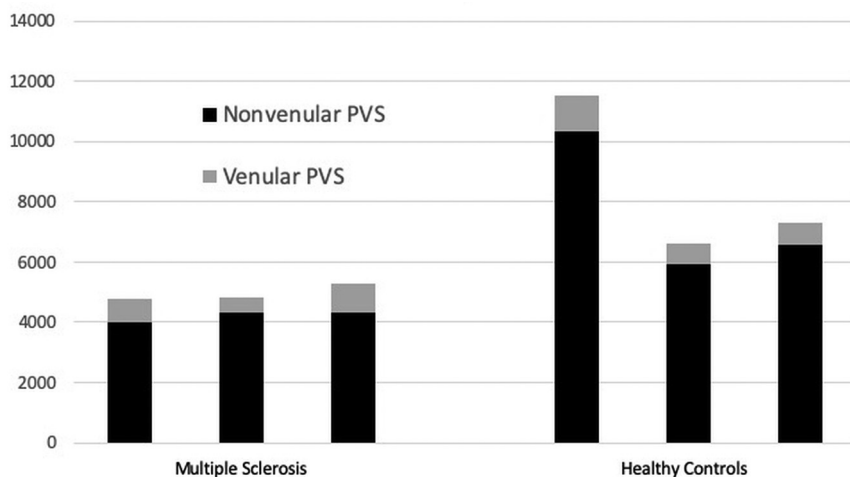
FIG 2. Nonvenular and venular PVS counts in 3 age-matched persons with MS and HC demonstrate more PVSs in HC but a higher proportion of venular PVSs in persons with MS. The number of nonvenular (black) and venular (dark gray) PVSs detected is depicted for each MS and healthy control subject.

group, the number of venular and total PVSs was independent of it ($\chi^2 = 99, 2\ df$).

DISCUSSION

We developed a method to identify venular PVSs using coregistered SWI-mapping deoxygenated blood signal and demonstrate the feasibility and reproducibility of this approach in the hemispheric white matter at 7T.

While our cohort is too small to draw definitive conclusions comparing persons with MS with HC, preliminary results suggest an increased proportion of venular PVSs in persons with MS. Furthermore, in HC, the venular PVS number was highly dependent on the total number of PVSs, while in persons with MS, these were independent ($P < .001$), implying that these differences are specific to this compartment and would not have been detected by analyzing total numbers or total volume of PVSs. We found lower numbers of total PVSs in persons with MS compared with HC; however, the difference was not statistically significant. The larger total PVS number found in our study suggests that previous findings at 1.5T may not extend to higher field strengths, which improve PVS detection. We plan to further explore these results in a larger cohort.

A recent meta-analysis demonstrated that enlarged PVSs are more prevalent in persons with MS versus HC, though study designs varied widely. No study differentiated venular and arteriolar PVSs.[4-6,14,15] The total number of PVSs detected in our study is greater than those previously reported at 7T,[12] likely due to differences in measurement algorithms. A larger study using our approach would clarify how the venular PVS number and size differ in MS and whether treatment modulates these changes.

Limitations of the current study include the small number of subjects and raters. We are refining a semi-automated method to measure PVSs at 7T to improve feasibility and interrater reliability. Additionally, PVSs within gray matter, the posterior fossa, and T2-hyperintense lesions were not included in the analysis due to difficulty of detection on TSE images.

Controlling for nonlesional brain volume normalizes the dataset to normal-appearing white matter and may mitigate the exclusion of PVSs from within lesions, though our method may be limited in subjects with large, confluent white matter lesions.

Future steps include the validation of preliminary findings from this study in a larger cohort and developing an automated tool to identify PVSs in a shorter timeframe than manual detection. Critical questions remain as to whether PVS anatomy corresponds to disease activity, active relapse, response to treatment, brain atrophy, neurodegeneration, and disability progression.

CONCLUSIONS

We present a semi-automated method of differentiating venular and nonvenular PVSs. The algorithm is reproducible and feasible in a group of persons with MS and HC and has the potential to identify an important biomarker in MS.

REFERENCES

1. Abbott NJ. **Astrocyte-endothelial interactions and blood-brain barrier permeability.** *J Anat* 2002;200:629–38 CrossRef Medline
2. Lassmann H. **Pathogenic mechanisms associated with different clinical courses of multiple sclerosis.** *Front Immunol* 2018;9:3116 CrossRef Medline
3. Kutzelnigg A, Lassmann H. **Pathology of multiple sclerosis and related inflammatory demyelinating diseases.** *Handb Clin Neurol* 2014;122:15–58 CrossRef Medline
4. Cavallari M, Egorova S, Healy BC, et al. **Evaluating the association between enlarged perivascular spaces and disease worsening in multiple sclerosis.** *J Neuroimaging* 2018;28:273–77 CrossRef Medline
5. Conforti R, Cirillo M, Saturnino PP, et al. **Dilated Virchow-Robin spaces and multiple sclerosis: 3 T magnetic resonance study.** *Radiol Med* 2014;119:408–14 CrossRef Medline
6. Wuerfel J, Haertle M, Waiczies H, et al. **Perivascular spaces–MRI marker of inflammatory activity in the brain?** *Brain* 2008;131:2332–40 CrossRef Medline

7. Sati P, Oh J, Constable RT, et al. NAIMS Cooperative. **The central vein sign and its clinical evaluation for the diagnosis of multiple sclerosis: a consensus statement from the North American Imaging in Multiple Sclerosis Cooperative.** *Nat Rev Neurol* 2016;12:714–22 CrossRef Medline

8. Thompson AJ, Banwell BL, Barkhof F, et al. **Diagnosis of multiple sclerosis: 2017 revisions of the McDonald criteria.** *Lancet Neurol* 2018;17:162–73 CrossRef Medline

9. Arrighi-Allisan A, George I, Rutland J, et al. **Comparison of Perivenular Spaces at 7 Tesla in Relapsing-Remitting Multiple Sclerosis Patients and Healthy Controls.** In: *Proceedings of the ISMRM 27th Scientific Meeting,* Montréal, Canada. May 11-16, 2019. Poster: 2817.

10. Feldman RE, Rutland JW, Fields MC, et al. **Quantification of perivascular spaces at 7T: a potential MRI biomarker for epilepsy.** *Seizure* 2018;54:11–18 CrossRef Medline

11. Steger C. **An unbiased detector of curvilinear structures.** *IEEE Trans Pattern Anal Machine Intell* 1998;20:113–25 CrossRef

12. Frangi AF, Niessen WJ, Vincken KL, et al. **Multiscale vessel enhancement filtering.** In: Wells WM, Colchester A, Delp S, eds. *Medical Image Computing and Computer-Assisted Intervention: MICCAI'98.* Springer; 1998:130–37

13. Schmidt P, Gaser C, Arsic M, et al. **An automated tool for detection of FLAIR-hyperintense white-matter lesions in multiple sclerosis.** *Neuroimage* 2012;59:3774–83 CrossRef Medline

14. Granberg T, Moridi T, Brand JS, et al. **Enlarged perivascular spaces in multiple sclerosis on magnetic resonance imaging: a systematic review and meta-analysis.** *J Neurol* 2020;267:3199–3212 CrossRef Medline

15. Kilsdonk I, Steenwijk M, Pouwels P, et al. **Perivascular spaces in MS patients at 7 Tesla MRI: a marker of neurodegeneration?** *Mult Scler* 2015;21:155–62 CrossRef Medline